Sensors and Materials, Vol. 31, No. 10 (2019) 3067–3073
MYU Tokyo

S & M 1993

Prediction of the Property of Colorimetric Sensor Array Based on Density Functional Theory

Haiyang Gu,[1,3*] Xingyi Huang,[2] Quansheng Chen,[1,2] Yanhui Sun,[1]
Chin Ping Tan,[1,4] ZhaoJun Wei,[3] and Riqin Lv[1]

[1]School of Bio and Food Engineering, Chuzhou University, Chuzhou 239000, China
[2]School of Food and Biological Engineering, Jiangsu University, Zhenjiang 212013, China
[3]School of Food Science and Engineering, Hefei University of Technology, Hefei 230000, China
[4]Department of Food Technology, Faculty of Food Science and Technology, Universiti Putra Malaysia, 43400, Malaysia

(Received July 17, 2019; accepted September 18, 2019)

Keywords: colorimetric sensor array, density functional theory, volatile organic compounds, sensor design

The importance of a rapid, sensitive, and selective colorimetric sensor array (CSA) for the discrimination of a wide range of food quality attributes has been recognized in the food industry. Here, the density functional theory (DFT) method at the B3LYP/LANL2DZ level was used to analyze the molecular reactions between a CSA and volatile organic compounds (VOCs). The energy gaps for iron phthalocyanine (FePc) binding to VOCs show that FePc-O_2 and FePc-N_2 have relatively smaller energy gaps; this causes the process of FePc binding to O_2 and N_2 through more than one pathway. Because of the binding energy, FePc is sensitive to N_2, followed by trimethylamine, propane, and acetone, whereas H_2S, ethanol, and ethyl acetate may not be sensitive to FePc. We suggest that the DFT-based method is useful for the theoretical design of CSAs and perhaps other sensors containing metal phthalocyanine.

1. Introduction

Freshness is one of the main indicators that reflect food quality attributes during storage, processing, marketing, and consumption. Spoilage is a complex process that makes food unacceptable or undesirable for consumers owing to the changes in sensory characteristics. In addition to its effect on sensory characteristics, the spoilage of food products probably causes serious illness and even death for consumers. Therefore, a rapid method of monitoring the changes in the quality of food products should be developed for the food industry. Volatile organic compounds (VOCs) are one of the most important indicators for detecting and evaluating food freshness. Each food product has a characteristic profile of VOCs during each stage of the entire food chain.

Over the previous decades, a series of traditional methods, such as gas chromatography-mass spectrometry (GC-MS),[(1)] and electronic nose (EN),[(2)] have been developed for the detection

*Corresponding author: e-mail: guhaiyang51@163.com
https://doi.org/10.18494/SAM.2019.2520

ISSN 0914-4935 © MYU K.K.

and evaluation of food quality. However, almost all of these methods are based on physical adsorption and van der Waals interactions, which are the least selective and weakest molecular interactions between sensors and analytes. Here, a novel sensor-based method [i.e., colorimetric sensor array (CSA)] is developed to detect VOCs from food or other sources. According to previous studies, this helpful method is proved to have both high sensitivity and high selectivity to VOCs. It shows enormous discriminatory power for similar molecules, such as 2-picoline and 3-picoline. Moreover, it is also 20000-fold more sensitive than the methods based on physical adsorption and van der Waals interactions in theoretical and experimental studies.[3] In addition to its high sensitivity and high selectivity, this method is essentially unresponsive to water from 2000 to 20000 ppm in an environment where GC-MS and EN are difficult to perform. Therefore, this method is regarded as helpful in detecting and evaluating the food quality for the food industry. In this paper, we therefore intend to provide a design strategy for a CSA at the molecular level for the rapid detection of VOCs in food.

2. Materials and Methods

2.1 CSA

The schematic diagrams of the reactions between the CSA and an analyte are shown in Fig. 1. A typical CSA composed of a series of metalloporphyrins and other dyes show sensitivity to VOCs.[4] The reactive sites of metalloporphyrin are the metal atom in the center of the porphyrin plane, which is in agreement with previous studies.[5,6] Figure 1(a) shows an image of the CSA before reacting with an analyte. After exposure to the analyte, the image landscape shows a small change compared with the original image, which is difficult to be discriminated with the naked eye, as shown in Fig. 1(b). Therefore, the difference image between the images obtained before and after exposure to the analyte is always required to obtain a unique fingerprint for each analyte. A typical difference image is produced by subtracting the before-reaction image from the after-reaction image, as shown in Fig. 1(c).

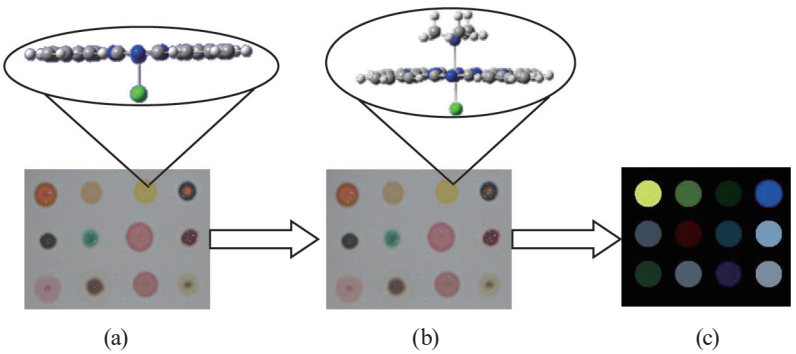

Fig. 1. (Color online) Schematic diagrams of CSA based on metalloporphyrin. Color images of the sensor array obtained (a) before and (b) after exposure to analyte. (c) Difference image obtained by subtracting the before-reaction image from the after-reaction image.

2.2 Computational method

The CSA model used is represented by a simple iron phthalocyanine (FePc) without any meso substituent. The initial unligated FePc and VOCs were obtained from the Cambridge Crystallographic Data Centre (CCDC). Each model consists of a planar phthalocyanin ring and the ligand lies along an axis perpendicular to the plane of the phthalocyanin ring. The FePc-VOC model was used to represented the CSA binding with an analyte by adding VOC molecules above the phthalocyanin ring at distances of 3–4 Å.[7] The FePc and a similar FePc-O_2 model are shown in Fig. 1. All calculations were implemented using Gaussian 09. Each model was calculated by applying the density functional theory (DFT) to B3LYP/LANL2DZ. The DFT-based method at this level was shown to be very efficient in the calculation of the geometries, energies, and charges of FePc and similar FePc complexes. To avoid any shortcomings, geometry optimization was carried out at three different spin states (low, intermediate, and high).[6]

3. Results and Discussion

3.1 Relative energy

According to a previous study,[8] all further calculations were carried out on the basis of the most stable geometry structure. The energy change associated with the geometry structures at three possible spin states (i.e., low-spin doublet, intermediate-spin quartet, and high-spin sextet) is the relative energy. The relative energy is the energy gap based on the most stable one. Figure 2 shows the relative energies for the FePc before and after exposure to different VOCs. It is important to note that FePc, FePc-H_2S, and FePc-$L_{1,4,5}$ have the most stable

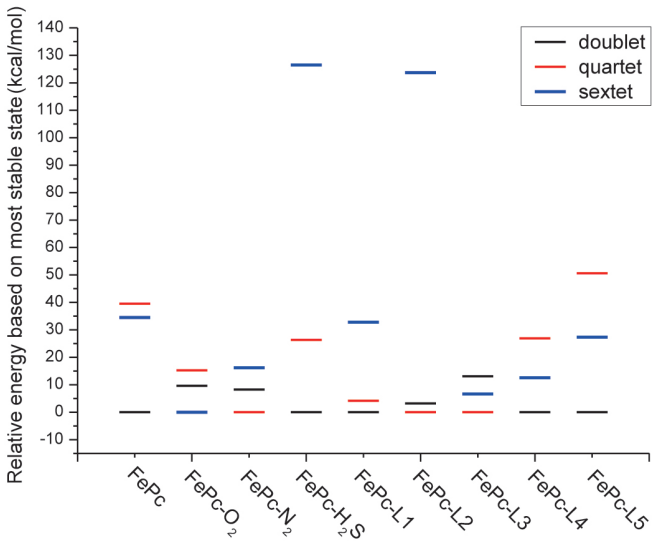

Fig. 2. (Color online) Relative energy obtained by subtracting the most stable energy from the unstable energy for each FePc and its complexes. L1 is trimethylamine, L2 is ethanol, L3 is propane, L4 is acetone, and L5 is ethyl acetate.

geometry structures at doublet, whereas FePc-N_2, FePc-$L_{3,4}$ and FePc-O_2 have the most stable geometry structures at quartet and sextet. In addition to the results of the analysis of the most stable geometry structures, the energy gaps between the most stable state and other states are observed to affect the binding capability of the FePc sensor. It is interesting to note that FePc-O_2, FePc-N_2, and FePc-$L_{1,2,3,4}$ have smaller energy gaps, and FePc-H_2S and FePc-L_5 have larger energy gaps. The smaller energy gaps probably mean that the binding process between the CSA and the VOCs is through more than one pathway, making the CSA react easily and more efficiently, as reported previously.[9]

3.2 Optimized molecular structure

All calculations were initiated from the appropriate geometry structures optimized at fixed spin multiplicity. Besides the effect of the geometry structure, the binding pattern also affects the capability of the CSA to bind VOCs. There are two binding patterns, the end-on[10] and side-on.[11] The end-on bent binding was proved to be well established by X-ray structure determination.[12] Furthermore, the side-on binding in the P450 model with a methyl mercaptide axial ligand for the heme iron had higher energy than the end-on bent binding with the O_2 geometry.[13] Therefore, the end-on pattern was selected to construct the FePc-VOCs. After optimizing the process, the molecular structures of FePc before and after exposure to VOCs were obtained and are shown in Fig. 3. The distances between the Fe atom in the center of the metalloporphyrin plane and the VOCs ranged from 1.996 to 4.143 Å, which is in agreement with the results of a previous theoretical study.[7] In Fig. 3, for the unligated metalloporphyrin, the distances of Fe-Cl are 2.245 Å for doublet, 2.349 Å for quartet, and 2.320 Å for sextet. It is clearly observed that the molecular structures were changed at the different spin states. As shown in Fig. 3, the Fe atom moved out of the metallophthalocyanine plane toward the VOCs. The complexes of FePc-VOCs showed a very interesting spin-structure relationship. Their distances are 0.019–0.156 Å for the doublet, 0.064–0.249 Å for the quartet, and 0.113–0.471 Å for the sextet. FePc-N_2 has the largest out-of-planarity because of its negative ion, which is consistent with a previous study.[14]

3.3 Mulliken charge analysis

The chemical reactions between the CSA and VOCs involve bond formation and bond breaking, which are closely related to the charge distribution. The relationship between the charge configurations of the metal and nitrogen atoms may affect the binding of the CSA to VOCs. Figure 4 shows the charge relationship between the Fe and nitrogen atoms. The FePc and FePc-VOCs show larger positive charges on Fe atoms and more negative charges on nitrogen atoms, which are reflected by FePc, FePc-$L_{2,5}$, and FePc-H_2S data points at the left top of the line. On the other hand, FePc and FePc-$L_{1,3}$ have larger negative charges on Fe atoms and more positive charges on nitrogen atoms at the lower right corner of the lines. It is interesting to note that the unligated FePc has the largest positive charge on the Fe atom, whereas FePc has the lowest positive charge. The reason for this may be that N_2 is a better electron donor than the

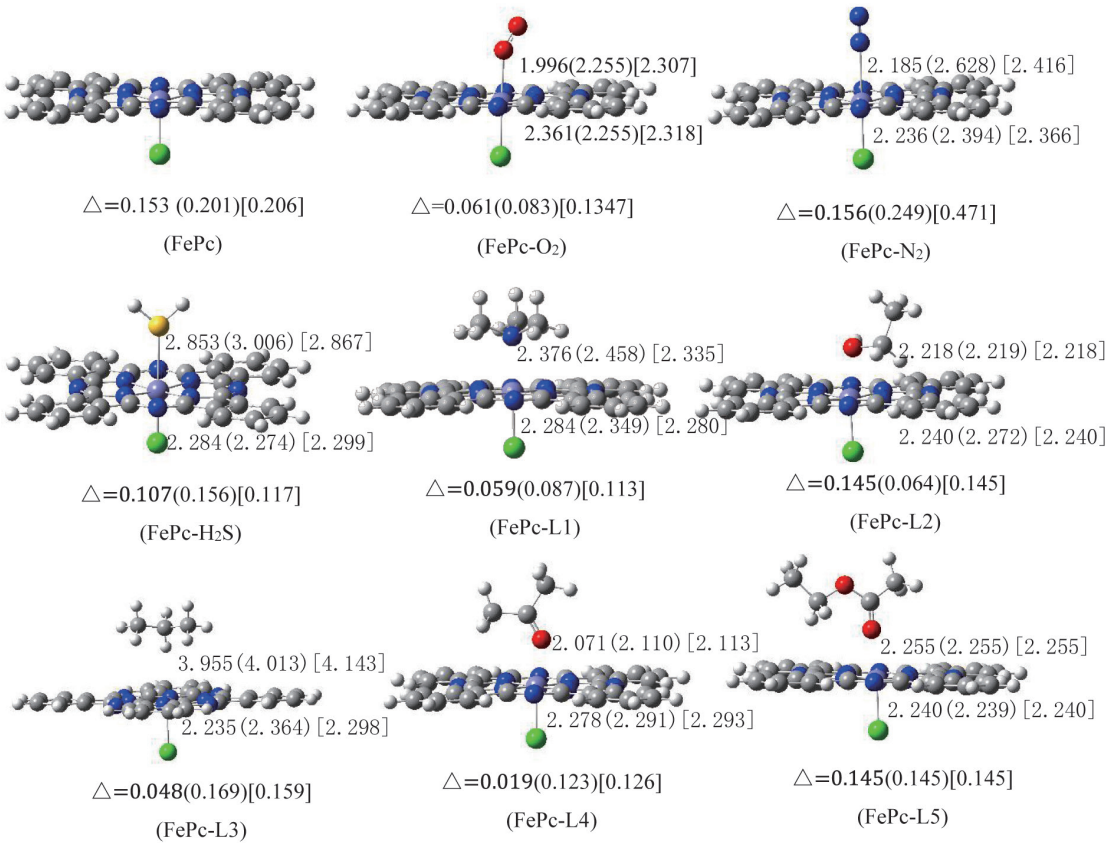

Fig. 3. (Color online) Optimized molecular structures for further calculation of FePc and its complexes. Δ is the distance between the Fe atom and the metalloporphyrin plane. Data for the singlet is without parentheses, triplet data is within the parentheses, and quintet data is within the brackets.

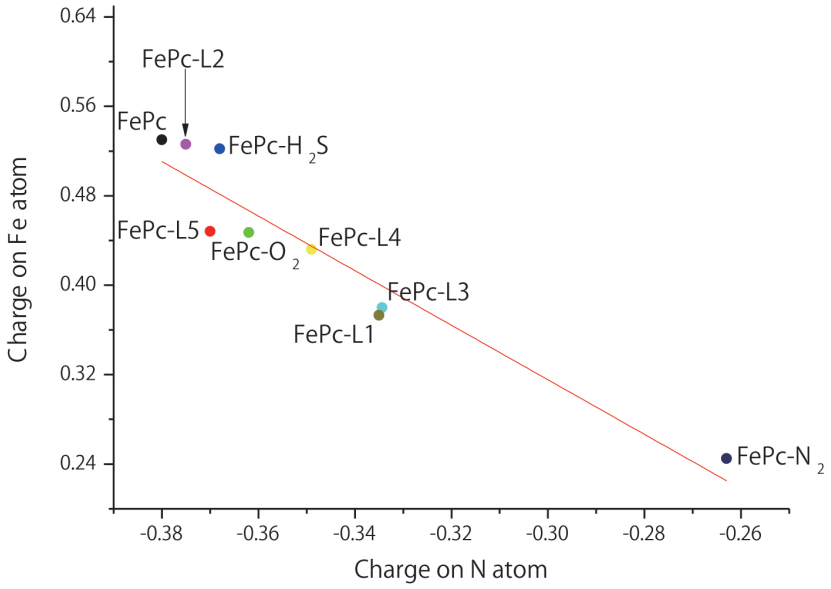

Fig. 4. (Color online) Strong linear relationships of charge distribution between Fe and N atoms in the center of the metalloporphyrin plane for different complex models.

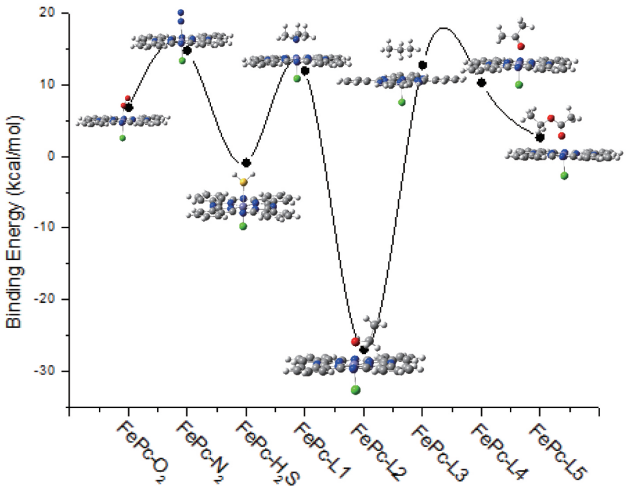

Fig. 5. (Color online) Binding energy of CSA for different VOCs.

others, which makes the Fe atom exhibit a more negative charge. When the VOC used is a good electron donor, there will be more electrons available in the metalloporphyrin system.

3.4 Binding energy

The reaction process between the CSA and the VOCs can be written as FePc + VOCs → FePc − VOCs. The energy change associated with the CSA before and after exposure to VOCs, which reflects the property for the binding of the CSA to different VOCs, was represented by binding energy (*BE*). After obtaining the energy of the CSA before and after exposure to VOCs, the binding energy can be calculated as $BE = E_{\mathrm{FePc}} + E_{\mathrm{VOCs}} - E_{\mathrm{FePc-VOCs}}$. Figure 5 shows the binding energy (kcal/mol) for all the FePc-VOCs. It is interesting to note that FePc-N_2 exhibits the largest binding energy, followed by FePc-$L_{1,3,4}$ and O_2, whereas FePc-$L_{2,5}$ and H_2S have relatively smaller binding energies. The reason for this may be that N_2 is a better electron donor than the others, making the Fe atom in the center of the metalporphyrin plane take the largest negative charge. However, L2 is not as good an electron donor as the others, which makes the Fe atom exhibit the largest positive charge. When the VOC used is a good electron donor, there may be higher binding energy through the reaction process between the CSA and the VOCs.

4. Conclusion

A DFT-based method for the design of a CSA with different VOCs was developed at the molecular level. This theoretical study was carried out at the B3LYP/LAN2DZ level on the basis of an optimized molecule. The sensitivity of the CSA for different VOCs was represented by binding energy. The binding energies of the CSA before and after exposure to VOCs were calculated to measure binding capability profiles as a sensitivity indicator of the CSA. The

analysis of binding energies indicated that FePc is sensitive to FePc-N_2, followed by L1, L3, L4, and O_2, whereas L2, L5, and H_2S may not easily react with FePc. This result suggests that the DFT-based method is feasible for the theoretical design of the CSA. This method may also be helpful for other types of sensor design. Further study is required to investigate other types of CSA containing metalloporphyrin or other molecules.

Acknowledgments

This study was sponsored by the National Natural Science Foundation of China (31671932), the National Natural Science Foundation of China (31701685), the Program of Study Abroad for Young Scholars (gxgwfx2019061), and the Science and Technology Program of Chuzhou (2019ZN006).

References

1 S. Lim, J. G. Lee, and E. J. Lee: Food Chem. **234** (2017) 81.
2 F. Sinesio, C. D. Natale, G. B. Quaglia, F. M. Bucarelli, E. Moneta, A. Macagnano, R. Paolesse, and A. D'Amico: J. Sci. Food Agric. **80** (2000) 63.
3 K. S. Suslick, N. A. Rakow, and A. Sen: Tetrahedron **60** (2004) 11133.
4 M. C. Janzen, J. B. Ponder, D. P. Bailey, C. K. Ingison, and K. S. Suslick: Anal. Chem. **78** (2006) 3591.
5 A. Debuigne, R. Poli, C. Jérôme, R. Jérôme, and C. Detrembleur: Prog. Polym. Sci. **34** (2009) 211.
6 A. Abdurahman and T. Renger: J. Phys. Chem. A **113** (2009) 9202.
7 B. Minaev: Spectrochim. Acta, Part A **60** (2004) 3213.
8 Y. Sun, X. Hu, H. Li, and A. F. Jalbout: J. Phys. Chem. C **113** (2009) 14316.
9 K. P. Jensen and U. Ryde: J. Biol. Chem. **279** (2004) 14561.
10 H. B. Gray: Bioinorganic Chemistry, R. Dessy, J. Dillard, and L. Taylor, Eds. (American Chemical Society, 1971) Chap. 17.
11 J. S. Griffith: Chemmedchem **235** (1956) 23.
12 B. Shaanan: Nature **296** (1982) 683.
13 H. Dube, B. Kasumaj, C. Calle, M. Saito, G. Jeschke, and F. Diederich: Angew. Chem. Int. Ed. **47** (2008) 2600.
14 Y. Sun, X. Hu, H. Li, and A. F. Jalbout: J. Phys. Chem. C **113** (2009) 14316.